IEEE Access
Multidisciplinary | Rapid Review | Open Access Journal

Received August 14, 2019, accepted August 21, 2019, date of publication August 30, 2019,
date of current version September 20, 2019.

Digital Object Identifier 10.1109/ACCESS.2019.2938552

Effects of Some Operation Parameters on the Performance of a Reservoir Computing System Based on a Delay Feedback Semiconductor Laser With Information Injection by Current Modulation

DIAN-ZUO YUE[1], ZHENG-MAO WU[1], YU-SHUANG HOU[2], AND GUANG-QIONG XIA[1]
[1]School of Physical Science and Technology, Southwest University, Chongqing 400715, China
[2]School of Science, Inner Mongolia University of Science and Technology, Baotou 014010, China

Corresponding authors: Zheng-Mao Wu (zmwu@swu.edu.cn) and Guang-Qiong Xia (gqxia@swu.edu.cn)

This work was supported in part by the National Natural Science Foundation of China under Grant 61575163, Grant 61775184, and Grant 61875167, and in part by the Postgraduate Research and Innovation Project of Chongqing Municipality under Grant CYB19087.

ABSTRACT Via a Santa Fe time series prediction task, the performance of a reservoir computing (RC) system based on a delay feedback semiconductor laser (SL) under current modulation is experimentally investigated and evaluated in detail. Experimental results show that some key operation parameters including the modulation index, the feedback ratio and the SL bias current, seriously affect the prediction performance of this RC system. By optimizing parameter settings, the degradation of the RC performance with the increase of the SL bias current can be efficiently alleviated, and the RC system can still realize a good performance with a NMSE smaller than 0.1 even for the SL biased at a high level of three times threshold current I_{th}. This research is an improvement to a previously experimental report in which such RC system can achieve a good performance only under a SL bias level near I_{th}.

INDEX TERMS Reservoir computing, semiconductor laser, delay feedback, current modulation, Santa Fe time series, prediction performance.

I. INTRODUCTION

Nowadays, novel computational paradigms have attracted widespread attention due to the increasing demand for massive information processing [1], [2]. Among these novel methods emerged in the past decades, recurrent neural network (RNN) is one of the most successfully neuro-inspired approaches. RNN is composed of a large number of artificial neurons with recursive connections, and thereby can efficiently perform time-dependent tasks such as speech recognition and time-series prediction [3]. However, properly training RNN is difficult due to the widely known problems of gradient vanishing and exploding [4], which partly limits its large scale deployment in practical application. This drawback can be overcome by reservoir computing (RC), which is originally known as echo state network and liquid state machine and is introduced at the beginning of 21st century [5], [6]. RC can significantly simplify the training procedure by adopting a fixed connection weights in a reservoir and only training the readout weights and has been successfully applied in some fields [7], [8]. For early-stage RC systems, the reservoir is made up by a network of a larger number of interconnected nonlinear nodes, which results in the hardware implementation of RC very challenging. In 2011, Appeltant *et al.* innovatively implemented a RC based on a simple nonlinear delay system [9], where the complex network is replaced by a single nonlinear element with delay feedback and the large number of nonlinear nodes are replaced by the virtual nodes distributed in a feedback loop. Compared with the earlier RC systems, this RC based on a single nonlinear node has a great advantage in hardware implementation. Since then, nonlinear delay RC systems receive more attention. In 2012, two optoelectronic delay RC experiments were carried out [10], [11], where the

The associate editor coordinating the review of this manuscript and approving it for publication was Shuihua Wang.

reservoir is constituted by a Mach-Zehnder modulator with optoelectronic feedback. In the same year, a RC system based on a semiconductor optical amplifier with optical feedback was implemented, and all-optical information processing can be realized [12]. Shortly afterwards, another all-optical RC system was proposed and experimentally investigated by Brunner *et al.* [13], in which the reservoir is made up of a semiconductor laser (SL) with optical feedback. This SL-based RC system possesses some unique virtues such as low energy consumption, high information processing rate, true parallelism and relatively easy hardware implementation, and it has been further explored in a few years [14]–[24].

For a SL-based RC system, the information can be injected into the reservoir via optical injection or current modulation. During the past few years, SL-based RC systems under optical information injection have been extensively studied [15]–[23], but few attentions are paid on SL-based RC systems under electrical information injection [13], [14], [24]. Comparatively speaking, a SL-based RC system with electrical information injection is relatively simpler than that with optical information injection in hardware implementation since the components related to optical injection are not required. Via a classification task, this SL-based RC system with electrical information injection was firstly proposed and preliminarily tested [13], and the experimental results showed that a good performance can be obtained only when the SL is biased at a small current range near its threshold but the performance will be degraded for the SL biased at a high current level. After considering that a wide operation range of the SL bias current is necessary towards practical applications for SL-based RC under current modulation, very recently, our group has numerically demonstrated that this RC system can achieve a good performance within a wide current range by optimizing some parameters [24].

In this work, we experimentally investigate a RC system based on an optical delay feedback SL under current modulation in detail. Via a Santa Fe time series prediction task, we evaluate the influences of some key parameters such as the modulation index, the feedback ratio, and the SL bias current on the RC performances, and the dependence of the RC performance on the system rest state is examined. By adopting optimized operation parameters, the RC system can realize a good prediction performance even for the SL biased at a high current of three times its threshold.

II. EXPERIMENTAL SETUP

Figure 1 shows our experimental setup. A distributed feedback semiconductor laser (DFB-SL) is taken as the nonlinear node of the reservoir, whose bias current and temperature is controlled by a laser controller (LC, ILX-Lightwave, LDC-3724C) with an accuracy of 0.01 mA and 0.01°C, respectively. The modulation signal is generated by an arbitrary waveform generator (AWG, Tektronix, AWG70001A, 1.5KSa/s-50GSa/s) with a 50 Ω output impedance. A Bias Tee (Picosecond, 5541A, 80 KHz-26 GHz) is used to combine the bias current and the modulation signal. The feedback

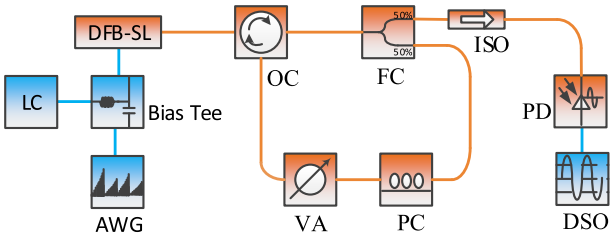

FIGURE 1. Experimental setup of a RC system based on an optical feedback SL under current modulation. DFB-SL: distributed feedback semiconductor laser; OC: optical circular; FC: fiber coupler; ISO: isolator; PD: photo-detector; PC: polarization controller; VA: variable attenuator; LC: laser controller; AWG: arbitrary waveform generator; DSO: digital storage oscilloscope.

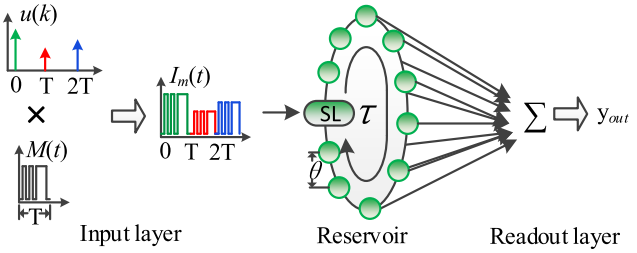

FIGURE 2. Schematic diagram of the operating principle for a RC system based on an optical feedback SL under current modulation.

loop is composed of an optical circulator (OC), a fiber coupler (FC), a polarization controller (PC), and a variable attenuator (VA). The PC keeps the polarization direction of the feedback light parallel with the emitted light, and the VA controls the feedback ratio. In the sampling section, an optical isolator (ISO) is utilized to suppress the unwanted reflection. The optical signal is converted into an electrical signal by a photo-detector (PD, New Forus, 1544-B, 12 GHz bandwidth). The electrical signal is recorded by a digital storage oscilloscope (DSO, Agilent, DSO-X 91604A, 40 GSa/s, 16 GHz bandwidth).

In this experiment, data pre-processing (masking in input layer) and post-processing (training and testing in output layer) are performed offline. Figure 2 is a schematic diagram to clearly illustrate the operating principle of the RC. As shown in the diagram, before original data $u(k)$ is fed into the reservoir, it is sampled with a period T (we set $T = \tau$, where τ is the delay time in feedback loop) and multiplied by a mask $M(t)$. The mask defines the coupling weights between input data and virtual nodes, it is a piecewise constant function with a period T and keeps a constant over an interval θ. To maximize the diversity of virtual node states, the mask is usually constituted by random sequences such as binary mask [25], [26], multi-level mask [27], and chaotic mask [28]. The mask used in this experiment is a binary mask, where the mask values are randomly extracted from $\{0.1, 1\}$ with equal probability. The masked data $I_m(t)$, *i.e.* the signal output by AWG, can be regarded as a continuous time signal which keeps a constant over θ [9], and it is fed into the reservoir serially to modulate the SL current. Under current modulation and optical feedback, the SL presents nonlinear

transient responses. The SL responses at different time are sampled and recorded for post-processing. In post-processing procedure, we define N virtual nodes distributed in a period τ with an interval θ. Then, N states of the virtual nodes can be collected within τ, and the state matrix $\mathrm{X}^{M\times N}$ of the reservoir is obtained after M successive τ. It should be noted that, in this experiment, the sampling rate of DSO is 40 GHz with a sampling step length of 0.025 *ns*. As a result, when the interval θ is larger than 0.025 *ns*, several sample points will be recorded in each θ. Here we define the virtual node states as the average of the sampling points around the middle of the corresponding time window over duration of $\theta/2$ [12].

The RC output is obtained by a linear combination of the virtual node states, *i.e.* $y_{out} = \mathrm{W}_{out}\mathrm{X}$, where W_{out} is the output weight and need to be optimized through training. During training process, the mean square error between the reservoir output y_{out} and the expected values y_d is minimized, and then $\mathrm{W}_{out} = (\mathrm{X}^{\mathrm{T}}\mathrm{X})^{-1}\mathrm{X}^{\mathrm{T}}y_d$ can be obtained via a standard regression algorithm.

III. RESULTS AND DISCUSSION

For successful information processing, a reservoir should fulfill some important properties including consistent responses, high-dimensional state space and fading memory [14], [29], which are related to the system dynamics. Previous studies have shown that an SL can exhibit rich nonlinear behaviors under external perturbation [30]–[33], and in this experiment the perturbations refer to feedback light and input signal. First, we focus on the variation of the system rest state (the system state without input data) with the feedback ratio k, where k is defined as a ratio of the feedback power and the output power of the DFB-SL at free-running.

During the experiment, the DFB-SL is stabilized at 20°C, and its threshold current I_{th} is about 8.50 mA at free-running. For a fixed bias current I_b, the SL can be entered into different dynamical states under optical feedback with different feedback ratio k. Figure 3 presents the temporal waveforms, power spectra and optical spectra of the SL under $I_b = 20$ mA and different k. For $k = -32$ dB (Row 1), the output power is nearly a constant with small ripples due to the noise, the optical spectrum is a typical single mode shape, and the power spectrum is similar to the noise floor. As a result, the SL can be determined to operate at a stable (S) state. For $k = -18$ dB (Row 2), the temporal waveform behaves a periodic oscillation, whose fundamental frequency is close to the relaxation oscillation frequency and is about 7.3 GHz obtained from the power spectrum. The optical spectrum presents multiple peaks with equal interval. All these features indicate that the SL operates at a period-one (P1) state. For $k = -15$ dB (Row 3), some new frequencies emerge around the fundamental frequency (6.5 GHz) and its harmonic frequency (13.0 GHz), which is the feature of a quasi-periodic (QP) state. As for $k = -12$ dB (Row 4), the time series fluctuates dramatically, the optical spectrum is broadened obviously, and the corresponding power spectrum continuously covers a very broad frequency range. Under this circumstance, the SL can be judged as a chaotic (C) state.

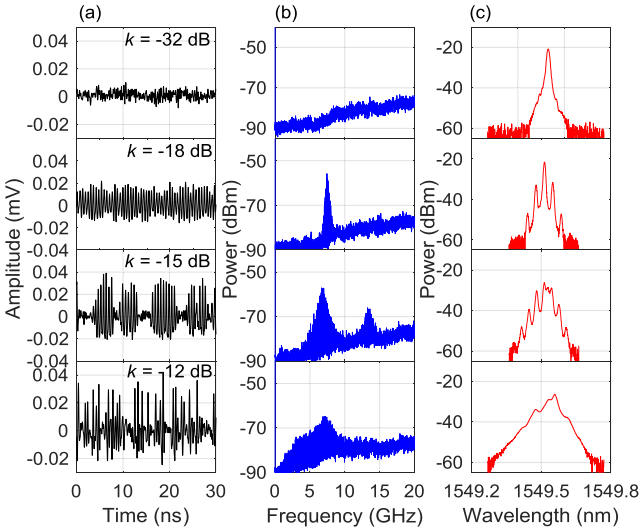

FIGURE 3. Temporal waveforms (Column a), power spectra (Column b), and optical spectra (Column c) of a SL under $I_b = 20$ mA and $k = -32$ dB (Row 1), $k = -18$ dB (Row 2), $k = -15$ dB (Row 3), and $k = -12$ dB (Row 4), respectively.

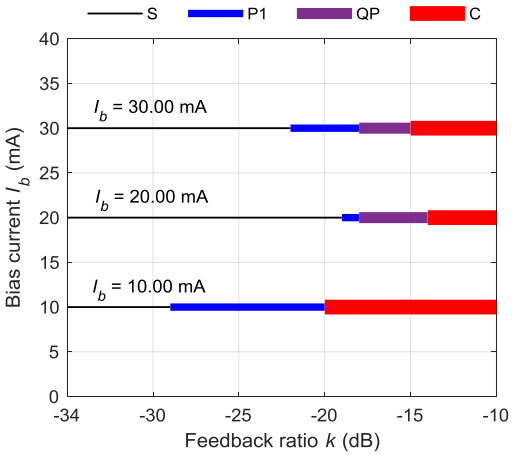

FIGURE 4. Variations of the system rest state with the feedback ratio k under three different SL bias current I_b of 10 mA, 20 mA and 30mA. S: stable state; P1: period-one state; QP: quasi-periodic state; C: chaotic state.

We choose three different cases of SL bias current I_b to present the continuous variation of the system rest state with k, and the results are shown in Fig. 4. For $I_b = 10.00$ mA, the SL is sensitive to optical feedback, it operates at a stable state only when k is smaller than -29 dB. In the range of -29 dB $\leq k \leq -20$ dB, the SL exhibits a period-one (P1) state. When k is further increased, the SL exhibits a chaotic state. In the case of $I_b = 20.00$ mA, the SL tends to be less sensitive to feedback and operates at a stable state until k is increased to -18 dB. When k is further increased, the SL sequentially presents P1, quasi-periodic (QP) state, and chaotic state. Similarly, as for the case of $I_b = 30.00$ mA, the SL operates at a stable state for $k \leq -22$ dB, and with

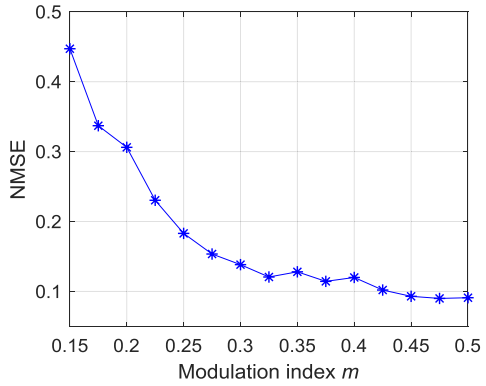

FIGURE 5. NMSEs as a function of m for $I_b = 20.00$ mA, $\theta = 0.2$ ns and $k = -28$ dB.

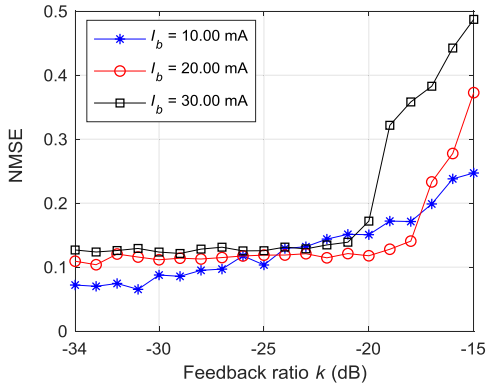

FIGURE 6. NMSEs as a function of k under three different cases of I_b for $\theta = 0.2$ ns and $m = 0.33$.

further increase of k the SL sequentially exhibits P1, QP and chaotic state. From this test, one can see that in the three cases of I_b, the system rest state undergoes a change from stable state to chaotic state with the increase of k, which will be helpful for assessing the relation between the RC performance and the system rest state in the following researches.

Next, we inject data into the reservoir to evaluate the performance of the RC system. Here, we select a benchmark task of Santa Fe time series prediction. The goal of this task is to predict the trajectory of a chaotic time series one step ahead the input data, where the chaotic time series are experimentally obtained from a far-infrared laser operating at chaotic state [34]. In this work, we use 3000 points for training and the subsequent 1000 points for testing. The prediction performance is quantified by the normalized mean square error (NMSE) between the reservoir output y_{out} and the expected values y_d. The NMSE can be expressed as:

$$\mathrm{NMSE} = \frac{1}{L}\sum_{n=1}^{L}(y_{out}(n) - y_d(n))^2/var(\mathrm{y}_d) \qquad (1)$$

where L is the total number of tested data, and var denotes the variance. In this research, the obtained NMSE is a mean value over four runs. NMSE = 0 indicates a perfect prediction while NMSE = 1 indicates a completely failed prediction. In general, for implementing a Santa Fe time series prediction task in hardware, a RC system with NMSE ≤ 0.1 is considered to be acceptable [16]. It is worth mentioning that very recently a RC system with a NMSE about 0.016 has been experimentally realized [35].

Since the data are electrically injected into the reservoir via directly modulating the SL current, the modulation index m as a key parameter may affect the prediction performance, where m is defined as I_m/I_b and I_m is the modulation current amplitude. In order to investigate the influence of m on NMSEs, we set the virtual node interval θ to 0.2 ns and choose a stable rest state as implemented in [13]. Under the case of $\theta = 0.2$ ns and a fixed delay time τ of 38.6 ns, there are 193 virtual nodes. The variation of NMSE with m for $I_b = 20.00$ mA and $k = -28$ dB is shown in Fig. 5. As shown in the diagram, for a small m of 0.15, the system yields a significantly bad performance of NMSE = 0.45. The NMSE decreases rapidly when m increases from 0.15 to 0.3 but decreases slowly when m is larger than 0.3. Obviously, under this circumstance, a relatively large m is helpful to improve the prediction performance. Taking into account the influence of m on NMSE and combining the maximum output amplitude of our used AWG, we set $m = 0.33$ in the following tests. Under this case, we can evaluate the RC performance within a range of $I_b \leq 30.00$ mA by adjusting the output amplitude of the AWG and without adding an electric amplifier.

In the above test, the prediction performance is analyzed under a stable rest state with $I_b = 20.00$ mA and $k = -28$ dB. Further, we investigate the dependence of the RC prediction performance on the system rest state. For convenience of comparison with Fig. 4, we still choose three different cases of I_b (10.00 mA, 20.00 mA, and 30.00 mA) and continually change k from -34 dB to -15 dB, and the results obtained under $\theta = 0.2$ ns and $m = 0.33$ are presented in Fig. 6. For $I_b =$ 10.00 mA, NMSEs fluctuate around 0.07 when $k < -30$ dB. Once k is larger than -30 dB (the system rest state is P1 as shown in Fig. 3), NMSEs gradually increase. In the cases of $I_b = 20.00$ mA and 30.00 mA, by comparing Fig. 4 and Fig. 6, NMSEs are maintained at a relatively low level when the system operates at a stable rest state, but NMSEs increase rapidly with k once the system operates at oscillated rest state. From this test, one can find that the prediction performance of the RC strongly depends on the system rest state. For the three different cases of bias current, relatively low prediction errors can be achieved under the system operating at stable rest state owing to that the system can generate consistently transient response. However, once the system presents oscillated rest state, its transient response will become more complicated under the stimulation of input data, which results in the degradation of prediction performance.

According to the results shown in Fig. 6, for $k = -31$ dB, NMSE obtained under three different I_b of 10.00 mA, 20.00 mA, and 30.00 mA is about 0.07, 0.11 and 0.13, respectively. It seems that a lower I_b will obtain a smaller NMSE. In order to identify the influence of I_b on NMSE,

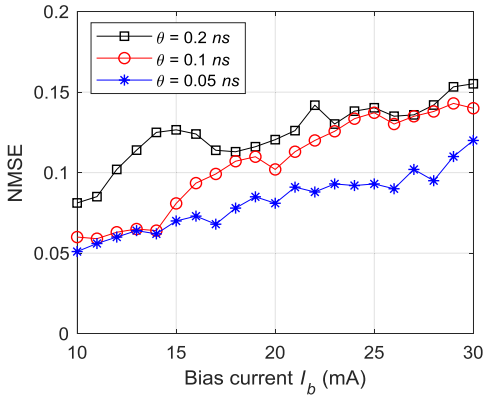

FIGURE 7. NMSEs as a function of I_b under three different cases of θ for $m = 0.33$ and $k = -31$ dB.

we continually change I_b from 10.00 mA to 30.00 mA with $m = 0.33$ and $k = -31$ dB. Meanwhile, considering that the virtual node interval θ also affects the RC performance, we choose three different cases of θ (0.2 *ns*, 0.1 *ns*, and 0.05 *ns*) to analyze the variation of NMSE with I_b. As shown in Fig. 7, the variations of NMSEs under three different θ present similar trends, *i.e.* NMSEs rise with fluctuations with the increase of I_b from 10.00 mA to 30.00 mA. For $\theta = 0.2$ *ns*, NMSEs increase from 0.08 to 0.16, and a good performance is realized only in the vicinity of the SL threshold current. In the case of $\theta = 0.1$ *ns*, NMSEs increase from 0.06 to 0.14, and a good performance can be obtained when $I_b \leq 17.00$ mA. As for $\theta = 0.05$ *ns*, NMSEs increase from 0.05 to 0.12, and I_b for yielding a good performance is enlarged to 27.00 mA (about three times threshold current). It can be concluded that under this experimental condition, a relatively low bias current is helpful to achieve a good prediction performance, which is due to better consistent response for SL biased at lower current [14]. Additionally, the performance degradation with the increase of I_b can be efficiently alleviated by adopting a short interval θ.

Finally, to intuitively illustrate the influence of the virtual node interval θ on the prediction performance, Fig. 8 displays corresponding results under $I_b = 10.00$ mA, where θ is set as 0.2 *ns* in Fig. 8(a) and 0.05 *ns* in Fig. 8(b), respectively. Obviously, the prediction errors for $\theta = 0.05$ *ns* are smaller than that for $\theta = 0.2$ *ns*. Additionally, we also test the RC performance under a shorter θ of 0.025 ns, but the prediction fails. The reasons for these experimental results may be explained as follows. A relatively short θ may increase the connectivity of the adjacent virtual nodes [9], [18] and results in a large N ($= \tau/\theta$), which is helpful to increase the state space dimension of the RC system. As a result, the prediction errors for $\theta = 0.05$ *ns* are smaller than that for $\theta = 0.2$ *ns*. However, as pointed out in Ref. [9], for a too short θ, too much averaging takes place and the RC system does not respond to the external input. Therefore, there exists an optimal value of θ, which is related to the relaxation oscillation frequency f_{ro} of the SL. It has been demonstrated that the SL-based

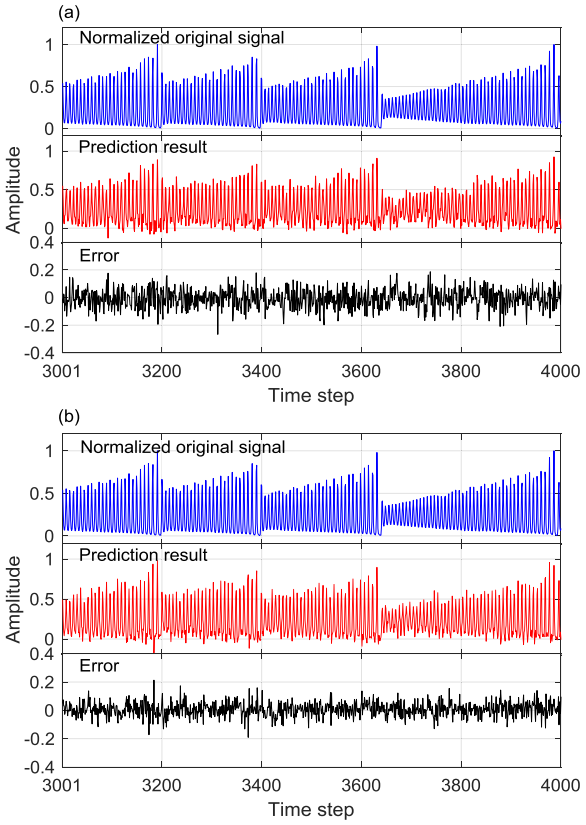

FIGURE 8. Experimental results of a Santa Fe time series prediction task under $I_b = 10.00$ mA, where (a) $\theta = 0.2$ *ns* and (b) $\theta = 0.05$ *ns*.

RC performs well when $\theta = 0.2T_{ro}$ ($T_{ro} = 1/f_{ro}$) [13], [24]. Since f_{ro} is about 3.3 GHz ($T_{ro} = 0.303$ *ns*) for $I_b = 10$ mA, the optimized value of θ is about 0.06 *ns*. Under this case, the obtained result under $\theta = 0.05$ *ns* (shown in Fig. 8(b)) is close to the optimized result.

IV. CONCLUSION

In summary, we experimentally investigate the influences of some key operation parameters on the performance of a RC system based on an optical feedback SL with information injection by current modulation. Via a Santa Fe time series prediction task, the influences of the modulation index, the feedback ratio and the SL bias current on the RC performance are assessed in detail. The relation between the system rest state and the RC performance is specified, and the optimal parameter settings are confirmed for realizing a good prediction performance. Experimental results show that under a modulation index of $m = 0.33$, a relatively low SL bias current is helpful to achieve a good RC performance, and a minimum NMSE of 0.05 is obtained in the vicinity of SL threshold current with a data processing rate of 25.9MSa/s. Moreover, though the prediction performance decreases with the increase of the SL bias current, the performance degradation can be efficiently alleviated by adopting a short virtual node interval of $\theta = 0.05$ *ns*. Under this case, the RC system can yield a good performance even under a high SL bias

current of three times its threshold. We believe that this research would be helpful to deeply understand the SL-based RC system under electrical information injection and then further exploit its potential applications.

REFERENCES

[1] J. P. Crutchfield, W. L. Ditto, and S. Sinha, "Introduction to focus issue: Intrinsic and designed computation: Information processing in dynamical systems—Beyond the digital hegemony," *Chaos, Interdiscipl. J. Nonlinear Sci.*, vol. 20, no. 3, Sep. 2010, Art. no. 037101.

[2] D. Woods and T. J. Naughton, "Optical computing: Photonic neural networks," *Nature Phys.*, vol. 8, no. 4, pp. 257–259, Apr. 2012.

[3] S. Hochreiter and J. Schmidhuber, "Long short-term memory," *Neural Comput.*, vol. 9, no. 8, pp. 1735–1780, Dec. 1997.

[4] Y. Bengio, P. Simard, and P. Frasconi, "Learning long-term dependencies with gradient descent is difficult," *IEEE Trans. Neural Netw.*, vol. 5, no. 2, pp. 157–166, Mar. 1994.

[5] H. Jaeger, "The 'echo state' approach to analysing andtraining recurrent neural networks—With an Erratum note," German Nat. Res. Center Inf. Technol., Berlin, Germany, GMD Rep. 148, 2001.

[6] W. Maass, T. Natschläger, and H. Markram, "Real-time computing without stable states: A new framework for neural computation based on perturbations," *Neural Comput.*, vol. 14, no. 11, pp. 2531–2560, Nov. 2002.

[7] H. Jaeger and H. Haas, "Harnessing nonlinearity: Predicting chaotic systems and saving energy in wireless communication," *Science*, vol. 304, no. 5667, pp. 78–80, Apr. 2004.

[8] A. Rodan and P. Tino, "Minimum complexity echo state network," *IEEE Trans. Neural Netw.*, vol. 22, no. 1, pp. 131–144, Jan. 2011.

[9] L. Appeltant, M. C. Soriano, G. Van der Sande, J. Danckaert, S. Massar, J. Dambre, B. Schrauwen, C. R. Mirasso, and I. Fischer, "Information processing using a single dynamical node as complex system," *Nature Commun.*, vol. 2, Sep. 2011, Art. no. 468.

[10] Y. Paquot, F. Duport, A. Smerieri, J. Dambre, B. Schrauwen, M. Haelterman, and S. Massar, "Optoelectronic reservoir computing," *Sci. Rep.*, vol. 2, no. 1, Feb. 2012, Art. no. 287.

[11] L. Larger, M. C. Soriano, D. Brunner, L. Appeltant, J. M. Gutierrez, L. Pesquera, C. R. Mirasso, and I. Fischer, "Photonic information processing beyond turing: An optoelectronic implementation of reservoir computing," *Opt. Express*, vol. 20, no. 3, pp. 3241–3249, 2012.

[12] F. Duport, B. Schneider, A. Smerieri, M. Haelterman, and S. Massar, "All-optical reservoir computing," *Opt. Express*, vol. 20, no. 20, pp. 22783–22795, Sep. 2012.

[13] D. Brunner, M. C. Soriano, C. R. Mirasso, and I. Fischer, "Parallel photonic information processing at gigabyte per second data rates using transient states," *Nature Commun.*, vol. 4, Jan. 2013, Art. no. 1364.

[14] K. Hicke, M. A. Escalona-Morán, D. Brunner, M. C. Soriano, I. Fischer, and C. R. Mirasso, "Information processing using transient dynamics of semiconductor lasers subject to delayed feedback," *IEEE J. Sel. Topics Quantum Electron.*, vol. 19, no. 4, Jul./Aug. 2013, Art. no. 1501610.

[15] H. Zhang, X. Feng, B. X. Li, Y. Wang, K. Y. Cui, F. Liu, W. B. Dou, and Y. D. Huang, "Integrated photonic reservoir computing based on hierarchical time-multiplexing structure," *Opt. Express*, vol. 22, no. 25, pp. 31356–31370, Dec. 2014.

[16] R. M. Nguimdo, G. Verschaffelt, J. Danckaert, and G. Van der Sande, "Simultaneous computation of two independent tasks using reservoir computing based on a single photonic nonlinear node with optical feedback," *IEEE Trans. Neural Netw. Learn. Syst.*, vol. 26, no. 12, pp. 3301–3307, Dec. 2015.

[17] J. Nakayama, K. Kanno, and A. Uchida, "Laser dynamical reservoir computing with consistency: An approach of a chaos mask signal," *Opt. Express*, vol. 24, no. 8, pp. 8679–8692, Apr. 2016.

[18] J. Bueno, D. Brunner, M. C. Soriano, and L. Fischer, "Conditions for reservoir computing performance using semiconductor lasers with delayed optical feedback," *Opt. Express*, vol. 25, no. 3, pp. 2401–2412, Feb. 2017.

[19] R. M. Nguimdo, E. Lacot, O. Jacquin, Q. Hugon, G. Van der Sande, and H. G. de Chatellus, "Prediction performance of reservoir computing systems based on a diode-pumped erbium-doped microchip laser subject to optical feedback," *Opt. Lett.*, vol. 42, no. 3, pp. 375–378, Feb. 2017.

[20] Y. Hou, G. Xia, W. Yang, D. Wang, E. Jayaprasath, Z. Jiang, C. Hu, and Z. Wu, "Prediction performance of reservoir computing system based on a semiconductor laser subject to double optical feedback and optical injection," *Opt. Express*, vol. 26, no. 8, pp. 10211–10219, Apr. 2018.

[21] X. Bao, Q. Zhao, H. Yin, and J. Qin, "Recognition of the optical packet header for two channels utilizing the parallel reservoir computing based on a semiconductor ring laser," *Mod. Phys. Lett. B*, vol. 32, no. 14, May 2018, Art. no. 1850150.

[22] Q. Zhao, H. Yin, and H. Zhu, "Simultaneous recognition of two channels of optical packet headers utilizing reservoir computing subject to mutual-coupling optoelectronic feedback," *Optik*, vol. 157, pp. 951–956, Mar. 2018.

[23] Y.-S. Hou, G.-Q. Xia, E. Jayaprasath, D.-Z. Yue, W.-Y. Yang, and Z.-M. Wu, "Prediction and classification performance of reservoir computing system using mutually delay-coupled semiconductor lasers," *Opt. Commun.*, vol. 433, pp. 215–220, Feb. 2019.

[24] D. Yue, Z. Wu, Y. Hou, B. Cui, Y. Jin, M. Dai, and G. Xia, "Performance optimization research of reservoir computing system based on an optical feedback semiconductor laser under electrical information injection," *Opt. Express*, vol. 27, no. 14, pp. 19931–19939, Jul. 2019.

[25] L. Appeltant, G. Van der Sande, J. Danckaert, and I. Fischer, "Constructing optimized binary masks for reservoir computing with delay systems," *Sci. Rep.*, vol. 4, no. 1, Jan. 2015, Art. no. 3629.

[26] M. Tezuka, K. Kanno, and M. Bunsen, "Reservoir computing with a slowly modulated mask signal for preprocessing using a mutually coupled optoelectronic system," *Jpn. J. Appl. Phys.*, vol. 55, Jul. 2016, Art. no. 08RE06.

[27] M. C. Soriano, S. Ortín, D. Brunner, L. Larger, C. R. Mirasso, I. Fischer, and L. Pesquera, "Optoelectronic reservoir computing: Tackling noise-induced performance degradation," *Opt. Express*, vol. 21, no. 1, pp. 12–20, Jan. 2013.

[28] Y. Kuriki, J. Nakayama, K. Takano, and A. Uchida, "Impact of input mask signals on delay-based photonic reservoir computing with semiconductor lasers," *Opt. Express*, vol. 26, no. 5, pp. 5777–5788, Mar. 2018.

[29] M. Hermans, M. C. Soriano, J. Dambre, P. Bienstman, and I. Fischer, "Photonic delay systems as machine learning implementations," *J. Mach. Learn. Res.*, vol. 16, pp. 2081–2097, Jan. 2015.

[30] A. Uchida, *Optical Communication with Chaotic Lasers: Applications of Nonlinear Dynamics and Synchronization*. Weinheim, Germany: Wiley, 2012, pp. 145–210.

[31] J. S. Lawrence and D. M. Kane, "Nonlinear dynamics of a laser diode with optical feedback systems subject to modulation," *IEEE J. Quantum Electron.*, vol. 38, no. 2, pp. 185–192, Feb. 2002.

[32] N. Li, R. M. Nguimdo, A. Locquet, and D. S. Citrin, "Enhancing optical-feedback-induced chaotic dynamics in semiconductor ring lasers via optical injection," *Nonlinear Dyn.*, vol. 92, no. 2, pp. 315–324, Apr. 2018.

[33] G.-Q. Xia, S.-C. Chan, and J.-M. Liu, "Multistability in a semiconductor laser with optoelectronic feedback," *Opt. Express*, vol. 15, no. 2, pp. 572–576, Feb. 2007.

[34] A. S. Weigend and N. A. Gershenfeld, *Time Series Prediction: Forecasting The Future And Understanding The Past*. Boston, MA, USA: Addison-Wesely, 1993. [Online]. Available: http://www-psych.stanford.edu/~andreas/Time-Series/SantaFe.html

[35] J. Vatin, D. Rontani, and M. Sciamanna, "Experimental reservoir computing using VCSEL polarization dynamics," *Opt. Express*, vol. 27, no. 13, pp. 18579–18584, Jun. 2019.

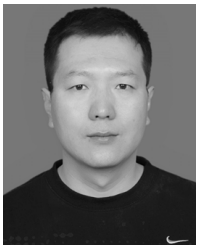

DIAN-ZUO YUE was born in Tangshan, Hebei, China, in 1982. He received the M.Sc. degree in information processing and automation from the Inner Mongolia University of Science and Technology, Baotou, China, in 2014. He is currently pursuing the Ph.D. degree in optics with Southwest University. His current research mainly focuses on the reservoir computing based on semiconductor lasers and its applications.

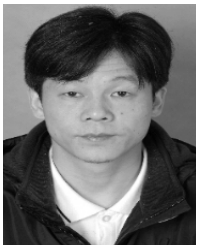

ZHENG-MAO WU was born in Wuyuan, Jiangxi, China, in 1970. He received the B.Sc., M.Sc., and Ph.D. degrees in optics from Sichuan University, Chengdu, China, in 1992, 1995, and 2003, respectively.

He is currently a Full Professor with the School of Physical Science and Technology, Southwest University, Chongqing, China. He has authored or coauthored more than 150 journal publications. His current research interests include the nonlinear dynamics of semiconductor lasers and their applications, chaotic semiconductor lasers and their applications, and photonic reservoir computing.

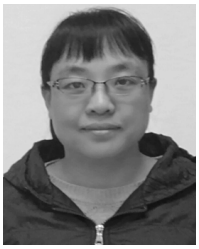

YU-SHUANG HOU was born in Tangshan, Hebei, China, in 1979. She received the M.Sc. degree in applied mathematics from Inner Mongolia University, Hohhot, China, in 2006, and the Ph.D. degree in optics from Southwest University, Chongqing, China, in 2019.

She is currently an Associate Professor with the School of Science, Inner Mongolia University of Science and Technology, Baotou, China. She has authored or coauthored more than ten journal publications. Her current research interests mainly focuses on the photonic reservoir computing and its applications.

GUANG-QIONG XIA was born in Fushun, Sichuan, China, in 1970. She received the B.Sc., M.Sc., and Ph.D. degrees in optics from Sichuan University, Chengdu, China, in 1992, 1995, and 2002, respectively.

She is currently a Full Professor with the School of Physical Science and Technology, Southwest University, Chongqing, China. She has authored or coauthored more than 160 journal publications. Her current research interests include the nonlinear dynamics of semiconductor lasers, synchronization and control of chaotic semiconductor lasers, chaos secure communication based on semiconductor lasers, microwave photonics, and photonic reservoir computing and its applications.